Scanning Microscopy

Volume 2 | Number 1 Article 3

9-13-1987

Impurity Lattice and Sublattice Location by Electron Channeling

S. J. Pennycook
Oak Ridge National Laboratory

Follow this and additional works at: https://digitalcommons.usu.edu/microscopy

Part of the Biology Commons

Recommended Citation
Pennycook, S. J. (1987) "Impurity Lattice and Sublattice Location by Electron Channeling," *Scanning Microscopy*: Vol. 2 : No. 1 , Article 3.
Available at: https://digitalcommons.usu.edu/microscopy/vol2/iss1/3

This Article is brought to you for free and open access by the Western Dairy Center at DigitalCommons@USU. It has been accepted for inclusion in Scanning Microscopy by an authorized administrator of DigitalCommons@USU. For more information, please contact digitalcommons@usu.edu.

Scanning Microscopy, Vol. 2, No. 1, 1988 (Pages 21-32) 0891-7035/88$3.00+.00
Scanning Microscopy International, Chicago (AMF O'Hare), IL 60666 USA

IMPURITY LATTICE AND SUBLATTICE LOCATION BY ELECTRON CHANNELING

S. J. Pennycook*

Solid State Division
Oak Ridge National Laboratory
Oak Ridge, Tennessee 37831-6024

(Received for publication March 16, 1987, and in revised form September 13, 1987)

Abstract

A new formulation is presented for the use of crystallographic orientation effects in electron scattering to determine impurity lattice location. The development of electron channeling techniques is reviewed and compared to high energy ion channeling and to the Borrmann effect in x-ray diffraction. The advantages of axial over planar geometry are discussed. Delocalization effects are more serious for quantitative analysis than have generally been believed. The new formulation applies to any crystal lattice and quantitatively includes delocalization effects via c-factors, which have been experimentally determined for diamond structure semiconductors. For sublattice site location this formulation removes the two major approximations of the original ALCHEMI formulation, namely that all the inner shell excitations are perfectly localized, and that all of the impurity atoms occupy distinct crystallographic sites. As an example, we study the location of small perfectly coherent Sb precipitates within the Si lattice.

KEY WORDS: axial channeling, planar channeling, atom location by channeling enhanced microanalysis, x-ray fluorescence, localization, substitutional fraction, semiconductors, dopants, impurities, precipitation.

*Address for correspondence:
S. J. Pennycook
Solid State Division
Oak Ridge National Laboratory
Oak Ridge, Tennessee 37831-6024
Phone No. (615) 574-5504

Introduction

The phenomena referred to as channeling occur when an incident wave or particle flux interacts strongly with the periodic potential of a crystal lattice. For high energy (MeV) electrons or ions the channeling is physical, that is, the particles are physically confined by the crystal potential, either to the channels in the case of positive ions, or to the atomic planes or strings in the case of electrons. For X rays and lower energy electrons (100 keV) the effect is best described in terms of dynamical diffraction where the photon flux or the electron wave intensity takes on the periodicity of the projected potential in the crystal. It is still useful to think of this behavior as effective channeling, since the distribution of total flux is clearly channeled even if it is not meaningful to think of single photons or electrons being channeled.

Associated with these channeling effects any close-encounter interaction would exhibit a large change in apparent cross section or yield depending on the extent of the channeling, which varies with the exact orientation of the incident beam relative to the crystal lattice. Provided a suitable close-encounter process can be found, these channeling effects can be used for studying the lattice location of impurity atoms in crystals. These ideas have been developed most extensively in the case of high energy ion channeling which is now a widely used experimental lattice location technique (Feldman et al., 1982). The close-encounter process employed is Rutherford backscattering, particularly for impurities heavier than the matrix; otherwise nuclear reactions or ion-induced x-ray emission can be used. With X rays, following a suggestion by Cowley (1964), the Borrmann effect (1941) has been employed for lattice location of bulk impurities (Batterman, 1969) and recently for atoms adsorbed on a crystal surface (Cowan et al., 1980).

In the case of medium energy electrons it has been known from the outset that the equivalent of the Borrmann effect occurs near Bragg reflections (Hirsch et al., 1962; Howie, 1966). This is responsible for the anomalous absorption effect in transmitted electron images (Hall and Hirsch, 1965) and the orientation dependence of other localized interactions such as x-ray

fluorescence (Duncumb, 1962; Hall, 1966; Cherns et al., 1973; Tafto, 1979; Bourdillon et al., 1981), and even visible cathodoluminescence shows a small orientation effect originating from localized energy transfers (Pennycook and Howie, 1980). These effects can all be successfully described by application of the dynamical theory of electron diffraction (Cherns et al., 1973). The first attempt to locate impurity atom sites appears to be due to Hall et al. (1966), who measured a change in the anomalous absorption of silicon crystals when As, B or Cu impurities were introduced. However, the sensitivity was low and detailed dynamical calculations were required. High-angle elastically scattered electrons are also sensitive to impurity atom sites, although again dynamical theory calculations are required (Treacy and Gibson, 1982; Pennycook et al., 1986). The breakthrough came when Tafto (1982) formulated a method for lattice location studies in crystals which was both sensitive, being based on x-ray fluorescence, and did not require dynamical theory calculations, since the channeling effect was calibrated by the x-ray fluorescence of the matrix itself. This formulation, later referred to as ALCHEMI (Atom Location by Channeling Enhanced Microanalysis, Spence and Tafto, 1982; Spence and Tafto, 1983), was essentially a sublattice location technique, restricted to compounds in which a planar or axial projection could be found consisting of two differently composed atomic planes or strings, and assumed that all the impurity atoms were in solution. The analysis determines the fraction of impurity contained in each type of plane or atomic string, and has found considerable application particularly to minerals (Spence et al., 1986). It has been generalized to situations where the distribution of the matrix constituents is unknown or altered by alloying (Krishnan and Thomas, 1984).

For a monatomic material such as silicon, Tafto et al. (1983) demonstrated using a quantitative measure of the orientation dependence for lattice location information, similar to the angular scans used in positive ion channeling (Feldman et al., 1982). Pennycook et al. (1984) showed that using spectra from just two orientations, a simple ratio technique similar to that used for ion channeling analysis could give a quantitative measurement of impurity substitutional fraction. Delocalization effects, though small, had to be accounted for in quantitative analysis using low-energy x-ray emission, and a simple way of doing so was proposed based on an experimentally determined correction to the channeling effect.

Axial-electron-channeling represents a powerful extension of these ideas (Pennycook and Narayan, 1985). An electron beam incident close to a zone axis simultaneously excites several low-index Bragg reflections, thus setting up standing waves in several directions simultaneously (Ichimiya and Lehmpfuhl, 1978). This results in the electron current being effectively channeled into columns, which, for electrons incident exactly at the zone axis, are located on the atomic strings as shown in Fig. 1. The electron current is well confined to the atomic

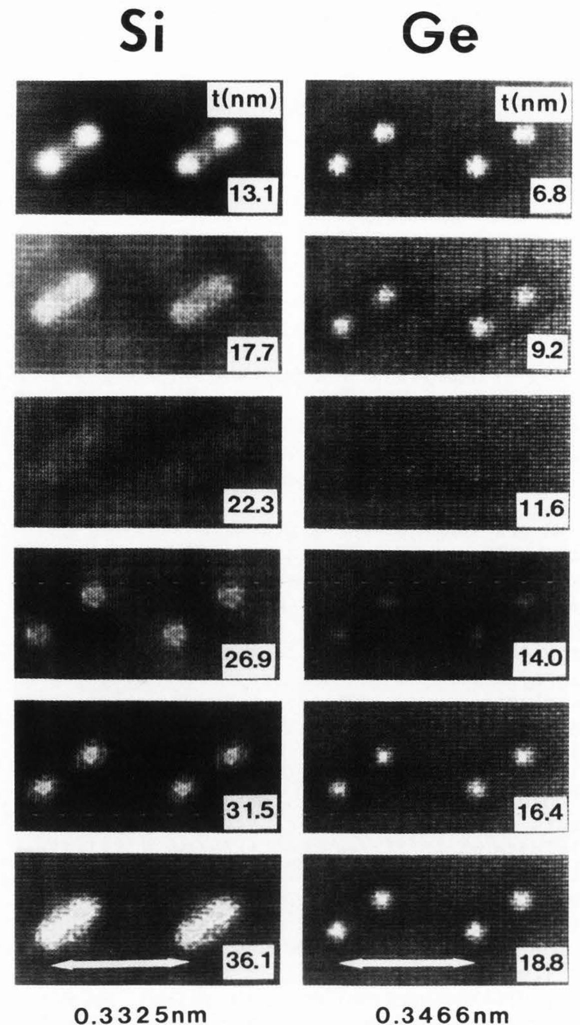

Fig. 1. Electron intensity distributions at various thicknesses in Si and Ge for 100 keV electrons incident along the exact <110> direction.

strings, rather more so in the case of Ge which has a higher scattering potential than Si. The distribution beats with a depth periodicity corresponding to the effective extinction distance in this high-symmetry orientation (Hirsch et al., 1977). Computations were done using 129 diffracted beams in a multislice calculation. (Computer programs were supplied by the Facility for High Resolution Electron Microscopy, Arizona State University, Tempe, AZ.) Recently, similar calculations have been performed by a real space method (Van Dyck, 1985).

The strong axial channeling effect results in a large enhancement of x-ray yield. Figure 2 compares the {220} planar and <100> axial-electron channeling of a supersaturated Si-As alloy in which the As is highly substitutional. Qualitatively at least the As and Si yields follow each other, and the channeling effect is much greater in the axial geometry. Since a quantitative analysis requires accurate measure of the difference between the two spectra, the

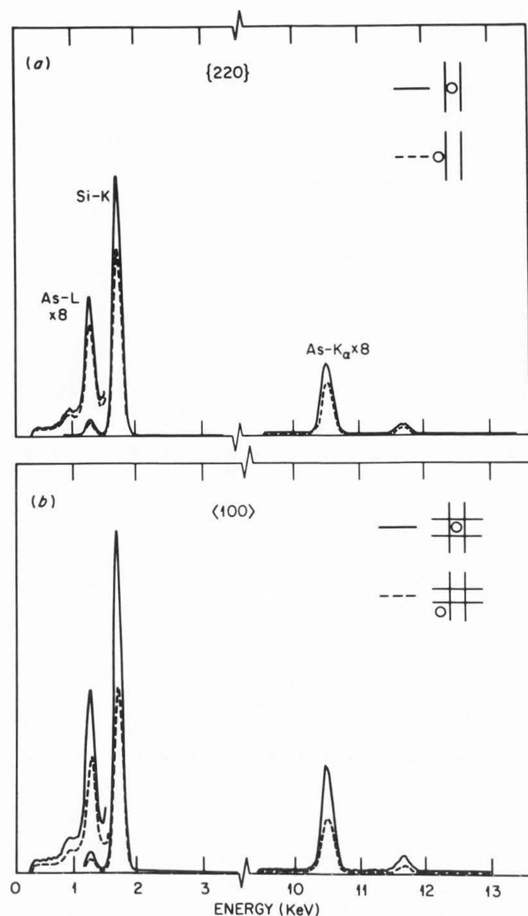

Fig. 2. X-ray spectra for {220} planar and <100> axial electron channeling of standard Si-As alloy showing enhanced channeling effect of axial geometry.

increased channeling effect for axial geometry gives better statistics, allowing higher sensitivity or shorter analysis times and reducing the effects of unintentional changes in experimental conditions. Delocalization effects must still be included for accurate analysis using low energy lines or small interplanar spacings. Bentley (1986) has extended the ALCHEMI formulation for sublattice site location to an axial geometry, and again delocalization corrections are required to avoid nonphysical results. A recent review on electron channeling has been given by Krishnan (1987).

In this paper a general formulation of electron channeling analysis is presented, based on measurements of the channeling effects of individual elements. Delocalization corrections are included by means of a correction to the channeling effect of each characteristic x-ray peak, referred to as a c-factor. This correction appears to follow a universal curve for the diamond-structure semiconductors and may be extendable to other lattice types. The formulation can be easily extended to sublattice determination, but avoids the two major assumptions of the original ALCHEMI formulation; delocalization corrections are included and impurity sites do not need to occupy a well defined lattice site in the matrix. Finally, as an illustration of these techniques, a study of a Si-Sb system is presented, in which part of the Sb is substitutional and part is in the form of interstitially located coherent precipitates.

Experimental Details

Each channeling measurement involves taking two x-ray fluorescence spectra from the same region with two different incident beam directions. For quantitative analysis one should be a good channeling condition and the other a good "random" orientation, where no strong low-order Bragg reflections are excited. If delocalization effects are important, the spectra should be recorded with the same incident beam current. The two orientations can be obtained either by tilting the specimen or by tilting the incident beam. Tilting the specimen can introduce errors due to the change in excited specimen volume, and the change in x-ray path length through the specimen. These are eliminated by tilting the incident beam, and repeatedly switching between the two tilt conditions will compensate for slow changes in beam current, or even for a slow build up of contamination which can quickly reduce the channeling effect. In axial geometry tilting the beam to a good random orientation requires a large beam tilt which introduces aberrations and changes the illuminated area of the specimen. This effect can be minimized by using equal and opposite tilts to switch between the two desired orientations.

Although collimated illumination is obviously required to observe channeling effects, the beam divergence can be surprisingly large. Figure 3 shows a "channeling effect map" for orientations around <100> in Si, taken on a VG Microscopes HB501 using a rocking incident beam and high-angle annular detector. Since high-angle elastic scattering is strongly localized, orientations of strong channeling show bright. This pattern is similar, but of opposite contrast, to the Kossel pattern observed in convergent beam diffraction (Ichimiya and Lehmpfuhl, 1978). There is little to be gained in reducing the incident beam semiangle much below the Bragg angle of the lowest order reflection. This is important for channeling studies using STEM, although higher convergence may be required for sublattice site location (Christenson and Eades, 1986; Tafto, 1983).

We have studied samples made by ion implantation of Si, when dopants can be incorporated substitutionally at concentrations greatly exceeding their solubility limit by various transient thermal processing techniques (White et al., 1980; Narayan et al., 1983). Several atomic % of Sb or As can be incorporated allowing good statistics to be obtained in analysis times of a few hundred seconds. The disadvantage of ion-implanted materials is that the dopant distribution may not be uniform. Central to the lattice location analysis is the idea that the matrix

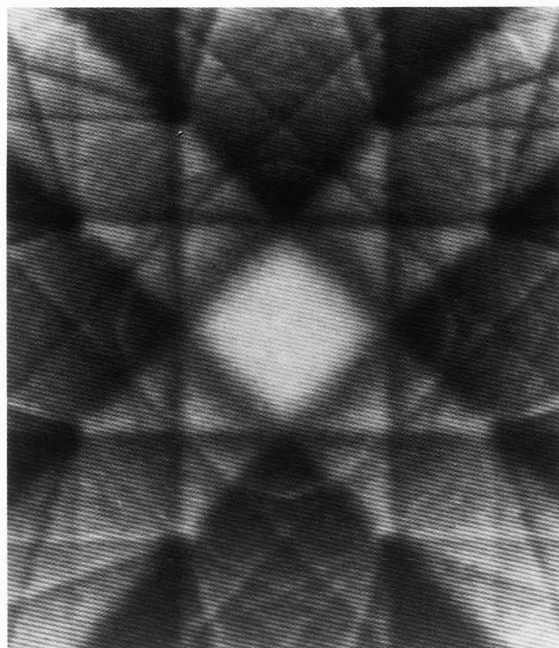

Fig. 3. A channeling effect map for electrons incident around <100> in Si obtained using a high-angle annular detector in STEM.

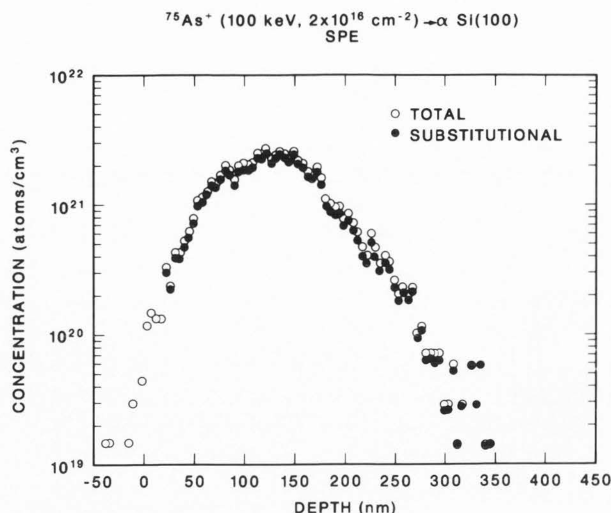

Fig. 4. Ion channeling analysis of standard Si-As sample obtained by ion implantation followed by solid-phase-epitaxial growth.

calibrates the channeling effect. Since the electron distribution shows strong depth periodicity (Fig. 1) the dopant must be uniformly distributed through the thickness of the specimen. Although single energy implantation results in a Gaussian depth profile (Fig. 4), using a cross section specimen, and a channeling direction reasonably close to the original sample surface, a uniform distribution of dopant through the sample thickness is automatically achieved. An approximately uniform depth profile can also be made by multiple energy ion implantation, and in this case plan view samples can be used. Experimentally, the effects of possible non-uniform impurity distribution can be assessed by simply inverting the specimen and repeating the channeling analysis.

All channeling analyses reported here were done in a Philips EM400T transmission electron microscope equipped with an Ortec EEDSII x-ray analysis system, and using the beam tilt method. Quantitation was done using computer programs of Zaluzec (1979) which accurately fit the shape of the Bremsstrahlung background. Areas of specimen approximately 50 nm in diameter and 100 nm in thickness were analyzed. Hole counts and absorption corrections were generally insignificant.

Formulation

The central feature to this formulation is the concept of channeling effect which is defined for each constituent and impurity element as the normalized change in x-ray count rate obtained on changing the incident beam from a channeling direction to a random direction. In a random condition the beam propagates as a plane wave and excites all atom locations equally. If N^C and N^R are the characteristic x-ray counts obtained from some region in the channeling and random conditions, respectively, then for the same beam current and analysis time, the channeling effect is simply:

$$\frac{N^C - N^R}{N^R} = \frac{N^C}{N^R} - 1 \quad . \tag{1}$$

Comparing the channeling effects of impurities and matrix is the basis of this lattice location method. Consider a monatomic matrix A where a fraction F_S of an impurity X is substitutional, and assume for the moment that the non-substitutional impurity is randomly located in the matrix, for example in precipitates which are not coherent along the channeling direction. The randomly located impurity will show no channeling effect, so the total impurity channeling effect is simply the fraction F_S of the matrix channeling effect, i.e.,

$$\left(\frac{N_X{}^C}{N_X{}^R} - 1\right) = F_S\left(\frac{N_A{}^C}{N_A{}^R} - 1\right)$$

and hence

$$F_S = \left(\frac{N_X{}^C}{N_X{}^R} - 1\right)/\left(\frac{N_A{}^C}{N_A{}^R} - 1\right) \quad . \tag{2}$$

The matrix calibrates the channeling effect and from each planar or axial channeling measurement a quantitative measure is obtained of the fraction of impurity atoms located within the matrix planes or atomic strings. Several measurements along different projections are

required to prove substitutionally, a procedure referred to as triangulation in ion channeling analysis. Atoms which appear substitutional in one direction but not in another are clearly in specific sites such as the tetrahedral or octahedral interstitial sites in Si. Again, a number of projections are required to solve a general lattice location problem, which can become quite complex. Information on structure and composition obtained by conventional microscopy techniques can be of great assistance (see example later) and is a clear advantage of using an electron microscope for channeling studies compared to an accelerator.

For a quantitative electron channeling analysis using low-energy x-ray lines delocalization effects must be quantitatively accounted for. In Si, the assumption of perfect localization is valid for x-ray lines in the 10 keV range, but is not valid for low-energy lines such as Si itself. It is not sufficient simply that a channeling effect be observed; it must be perfectly localized, or corrected in some way to the value it should have for perfect localization. The low-energy limit to channeling analysis based on x-ray fluorescence may not be as low as has been sometimes supposed (Self and Buseck, 1983). Analysis of light elements can be done using electron energy loss spectroscopy, in which there is independent control of scattering angle and therefore localization (Spence et al., 1982; Tafto and Krivanek, 1982).

An estimate of the impact parameter b, for transfer of energy ΔE from an electron of velocity v, based on classical (Jackson, 1975) or uncertainty principle (Craven et al., 1978) arguments gives $b = \hbar v/\Delta E$. Using the angular distribution of inelastic scattering, and integrating over all angles, the uncertainty principle argument has been extended to give an estimate of the root mean square impact parameter for x-ray excitation at threshold,

$$b^{RMS} = \frac{\hbar v}{\Delta E}\left[\ln\left(\frac{4E}{\Delta E}\right)\right]^{-1/2} , \qquad (3)$$

where E is the fast electron energy (Pennycook, 1982). This expression, which gives similar values to more recent estimates (Bourdillon, 1984) indicates $b^{RMS} = 0.025$ nm for Si-K excitation by 100 keV electrons. This is 1/8 of the {220} interplanar spacing, and although this is high localization it is not perfect, and the channeling effect is smaller than is observed for higher energy excitations. This reduction due to localization has been measured experimentally using standard samples (see next section) and is by a factor dependent only on b^{RMS} and the channeling condition. We have proposed that this factor, referred to as a c-factor, can be used to correct an experimentally measured channeling effect for small delocalization effects (Pennycook et al., 1984). The channeling effect measured experimentally depends on many additional factors including crystal perfection, thickness, the exact orientation, and the impurity substitutional fraction, but it can be simply scaled by the appropriate c-factor to quantitatively correct for the effects of delocalization. Equation (2) therefore becomes:

$$F_S = \frac{1}{c_X}\left(\frac{N_X{}^C}{N_X{}^R} - 1\right) \Big/ \frac{1}{c_A}\left(\frac{N_A{}^C}{N_A{}^R} - 1\right) . \qquad (4)$$

This formulation for a monatomic matrix can be simply extended to compounds or alloys where the projected structure along the channeling direction consists of two different atomic planes or strings, denoted by A and B. An impurity X now has a substitutional fraction for each sublattice, i.e.,

$$F_S = F_A + F_B , \qquad (5)$$

and the total impurity channeling effect is now given by

$$\frac{1}{c_X}\left(\frac{N_X{}^C}{N_X{}^R} - 1\right) = F_A\frac{1}{c_A}\left(\frac{N_A{}^C}{N_A{}^R} - 1\right) + F_B\frac{1}{c_B}\left(\frac{N_B{}^C}{N_B{}^R} - 1\right) ,$$

where small delocalization effects are included via c-factors as before.

Then:

$$F_A = \frac{\frac{1}{c_X}\left(\frac{N_X{}^C}{N_X{}^R} - 1\right) - F_S\frac{1}{c_B}\left(\frac{N_B{}^C}{N_B{}^R} - 1\right)}{\frac{1}{c_A}\left(\frac{N_A{}^C}{N_A{}^R} - 1\right) - \frac{1}{c_B}\left(\frac{N_B{}^C}{N_B{}^R} - 1\right)} . \qquad (6)$$

If a projection can be found with only one type of matrix plane or atomic string containing both A and B, then F_S can be determined using Eq. (4) and the sublattice occupancies are then given by Eq. (6). The c-factors are again experimentally determined, and in principle could be different for different channeling axes. If the same assumptions are made as in the original ALCHEMI formulation, that $F_A + F_B = 1$ and $c_X = c_A = c_B = 1$, then Eq. (6) reduces to Eq. (6) of Spence and Tafto (1983), where their orientations (1) and (2) represent our channeling and random orientations respectively.

Determination of c-factors

Standard samples of supersaturated Si-As and Si-Sb alloys were characterized by ion channeling analysis and used to determine the c-factors for electron channeling analysis. We assume that in the Si matrix excitations of $\Delta E \gtrsim 10$ keV are perfectly localized, since b^{RMS} is then $\lesssim 0.03$ of the {220} interplanar spacing. The simplest determination of a c-factor is obtained for an element which has a high energy K line and a low energy L line. The ratio of the channeling effect of the L line to that of the K line (the

right hand side of Eq. 2) directly gives the c-factor for the L line. In this way the As-L c-factor was determined using the standard Si-As sample. The c-factor for Si-K was obtained from the same spectra by applying Eq. (4), using the value of F_s = 0.95 determined by the ion channeling analysis (Fig. 4). The same procedure with the standard Si-Sb alloys gave values of C = c_{Sb}/c_{Si}. Figure 5 shows these c-factors as a function of ΔE, taken as the inner shell binding energy, and show clearly the onset of strong delocalization corrections at low energies where $d/b^{RMS} \lesssim 5$. Values for <100> axial and {220} planar channeling in Si are very close, and the solid line in Fig. 5 should give quite accurate c-factors for any impurity in Si and any channeling condition involving {220} reflections. Also shown is the c-factor for Ge-L, obtained from a sample of Ge, which also lies right on the curve. This is somewhat surprising in view of Fig. 1, which indicates the electron current to be confined closer to the atomic strings in Ge than Si, and therefore delocalization corrections would be expected to increase. However, the actual electron distributions are probably broadened by localized elastic and inelastic scattering processes, so that the only major difference between Si and Ge may well be just the depth periodicity. It seems most likely that Fig. 5 will give c-factors for all the diamond structure semiconductors, since they have very similar lattice parameters. It may also be possible to predict c-factors for other beam voltages or interplanar spacings using the upper axis of d/b^{RMS} where d is the interplanar spacing of the lowest order reflection contributing to the channeling.

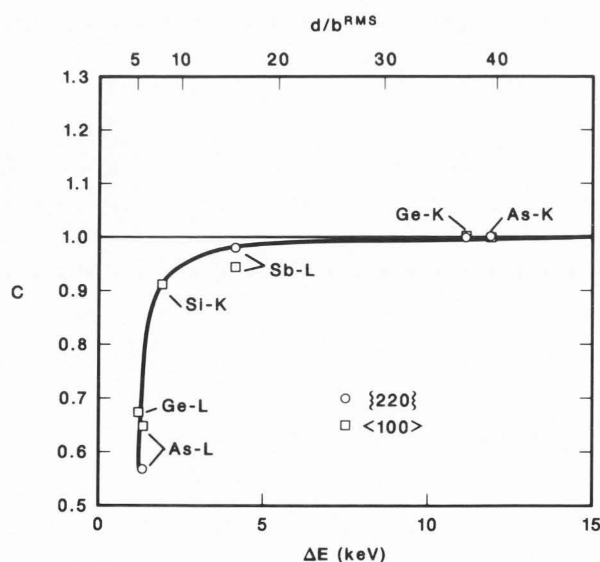

Fig. 5. Experimentally determined c-factors for delocalization correction of channeling effects.

Sb precipitation - a case study

A supersaturated Si-Sb alloy provides an ideal test of the quantitation procedure since all the Sb in excess of the solubility limit can be precipitated by annealing. The standard sample formed by multiple implantation had an approximately uniform Sb concentration of 8.8×10^{20} cm^{-3} from 10 to 110 nm in depth and by suitable annealing F_s values ranging from ~1 to ~0.05 could be obtained. Table 1 compares results of {220} electron channeling obtained from regions 110 nm thick, with <110> ion channeling measurements obtained by integrating over a depth window of 10-110 nm. Excellent quantitative agreement was obtained using the c-factors shown in Fig. 5 for the electron channeling analysis. An independent measure of precipitated fraction was also obtained from the size distribution observed in TEM micrographs, using the known total concentration and the width of the precipitate band observed in cross section samples. Precipitates could be observed even with a random beam orientation, and the size distributions showed clear peaks well above the visibility limit. Therefore all precipitates are thought to be visible, but the precipitated fraction could not account for the channeling measurements. A more detailed study was performed by sequentially annealing one sample, and Fig. 6 shows a plot of the apparent nonsubstitutional fraction determined by {220} electron channeling versus the precipitated fraction. Good quantitative agreement is obtained when most of the Sb has been precipitated. The discrepancies at low precipitated fractions are believed to be caused by coherency of the small Sb precipitates. If coherency was such that matrix and precipitate planes were aligned, the Sb in precipitates would appear substitutional to a channeling measurement. The reverse effect observed here indicates that the precipitate planes are interstitially located between the Si planes. The precipitated Sb would contribute to the random spectrum, but would show a reduced yield under a channeling condition, hence reducing the measured total channeling effect. A similar effect occurs in ion channeling, where interstitial atoms give enhanced scattering yields due to flux peaking (Anderson et al., 1971). Hence, the electron and ion channeling can both agree but be in error.

The large discrepancy can only be explained if the precipitated Sb is fully coherent with the Si lattice. A partial coherency has been found

Table 1
Comparison of nonsubstitutional fraction of Sb determined by electron and ion channeling, and precipitated fraction of Sb in Si-Sb alloy annealed for 20 min at various temperatures.

Annealing temperature °C	Nonsubstitutional fraction by channeling using electrons	ions	Precipitated Fraction
720	0.41±.04	0.42	0.18
740	0.49±.04	0.48	0.26
780	0.57±.05	0.59	0.46

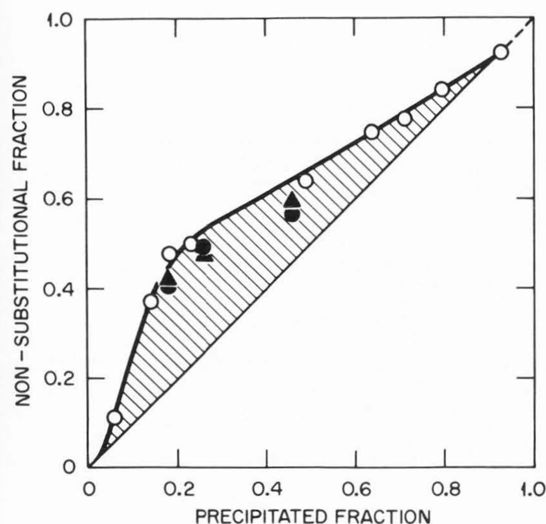

Fig. 6. Plot of apparent nonsubstitutional fraction measured by electron (circles) or ion (triangles) channeling vs precipitated fraction in annealed Si-Sb alloy standard. Solid and open symbols denote samples annealed in bulk or thinned form, respectively.

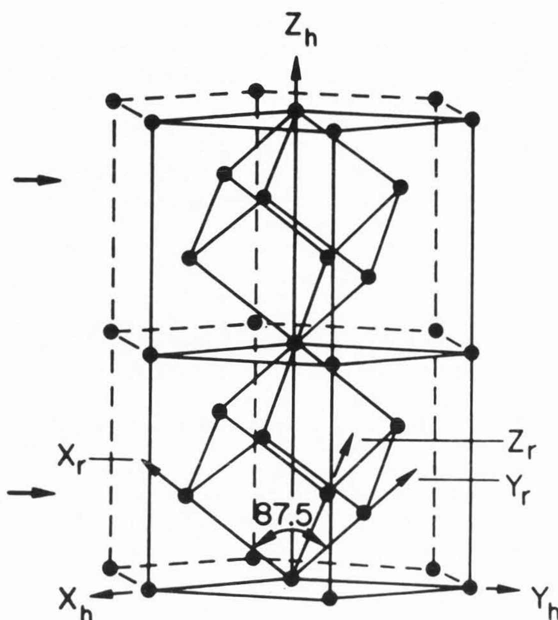

Fig. 7. Relation between the hexagonal cell of $R\bar{3}m$ Sb and a smaller rhombohedral cell, see text.

for large Sb precipitates, which were identified to be the trigonal $R\bar{3}m$ phase of Sb with $\{\bar{1}012\}$ Sb coherent with $\{111\}$ Si (Pennycook et al., 1983). In fact the trigonal structure is quite close to simple cubic as illustrated in Fig. 7, and it is quite possible that a higher coherency could occur for smaller precipitates. The planes arrowed in Fig. 7 are displaced along the Z_h axis by small but different amounts. If it was not for this displacement, the structure could be described by the smaller rhombohedral unit cell, where the $\{100\}$ plane of the rhombohedral cell is equivalent to the $\{\bar{1}012\}$ plane of the hexagonal cell. Complete coherency would result if these $\{100\}$ "cube" planes with 0.311 nm spacing could be coherent with the $\{200\}$ Si planes, which have a spacing of 0.272 nm. The precipitates may even have transformed to the high pressure simple cubic phase, which has a lattice parameter of 0.295 nm (Berry, 1981).

Whether the precipitates have transformed or not, it is simple to understand the origin of the interstitial coherency. Figure 8 shows one unit cell of the (100) Si surface with 4 unit cells of the coherent (100) Sb surface superposed, but with the origin displaced from the origin of the Si cell by $\frac{a}{4}\langle 100\rangle Si = \frac{a}{2}\langle 100\rangle Sb$ in order to avoid superposing Si and Sb sites. Now perfect coherency is achieved, but with all Sb atoms interstitially located with respect to the $\{220\}$ Si planes. In reality the displacement vector $\underline{R}$ between the origins of the two cubic cells will be in three dimensions so as to minimize the total surface energy of all the coherent precipitate interfaces. The simple displacement of Fig. 8, though illustrating the idea, predicts the Sb would look substitutional to $\{400\}$ planar channeling whereas experimentally it does not.

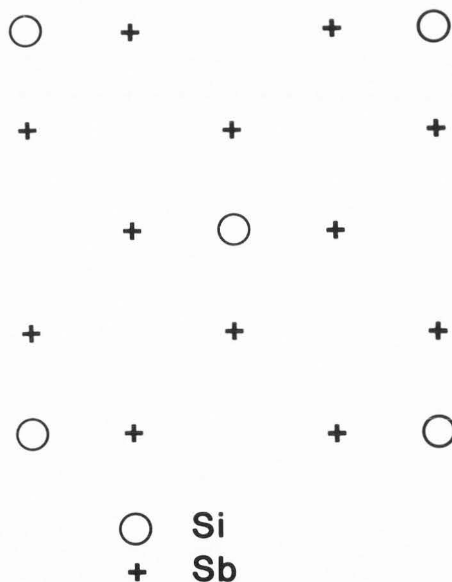

Fig. 8. Illustration of a possible interstitial coherency between (100)Si and (100)Sb surfaces.

Careful measurements of a number of planes and axes are under way to determine the coherency displacement vector $\underline{R}$.

Conclusions

A new formulation has been presented for electron channeling analysis based on measuring channeling effects of individual elements. It is applicable to monatomic or compound materials to determine total and sublattice substitutional fractions. Small delocalization effects are shown to be important for quantitative analysis and can be quantitatively accounted for via experimentally determined c-factors. These have been determined for channeling involving {220} reflections in diamond structure semiconductors, and may be applicable to other systems. In many materials, axial channeling gives enhanced channeling effects and is highly advantageous compared to planar channeling. The formulation has been applied to Si-Sb alloys containing Sb precipitates, demonstrating good agreement between ion and electron channeling analysis, but that both disagree with an independent measurement of precipitated fraction. This is explained as resulting from perfect coherency of small Sb precipitates, which is of interstitial rather than substitutional type. To minimize interfacial energy, a rigid translation of the coherent Sb lattice occurs.

Acknowledgments

The author is grateful to P. E. Batson and W. Krakow for assistance in obtaining Fig. 3, to R. J. Culbertson for the ion channeling analysis of Fig. 4, to J. Bentley and J. Narayan for stimulating discussions, and to J. C. H. Spence for bringing important references to his attention. This research was sponsored by the Division of Materials Sciences, U.S. Department of Energy under contract DE-AC05-84OR21400 with Martin Marietta Energy Systems, Inc.

References

Anderson JU, Andreasen O, Davies JA, Uggerhoj E (1971). The use of channeling-effect techniques to locate interstitial foreign atoms in silicon. Radiat. Eff. 7 25-34.

Batterman B (1969). Detection of foreign atom sites by their x-ray fluorescence scattering. Phys. Rev. Lett. 22 703-705.

Bentley J (1986). Site occupations in $L1_2$ ordered alloys by axial electron channeling microanalysis. 44th Proc. EMSA, (ed) GW Bailey, San Francisco Press, 704-705.

Berry LG (1981). (Ed) Powder Diffraction File, JCPDS International Center for Diffraction Data, Swarthmore, PA, Card 17-125.

Borrmann G (1941). Über Extinktionsdiagramme von Quarz. Phys. Z. 42 157-162.

Bourdillon AJ, Self PG, Stobbs WM (1981). Crystallographic orientation effects in energy dispersive x-ray analysis. Phil. Mag A 44 1335-1350.

Bourdillon AJ (1984). The measurement of impact parameters by crystallographic orientation effects in electron scattering. Phil. Mag. A50 839-848.

Cherns D, Howie A, Jacobs MH (1973). Characteristic x-ray production in thin crystals. Z. Naturforsch. 28a 565-567.

Christenson KK, Eades JA (1986). On parallel illumination conditions for ALCHEMI. 44th Proc. EMSA, (ed) GW Bailey, San Francisco Press, 622-623.

Cowan PL, Golovchenko JA, Robbins MF (1980). X-ray standing waves at crystal surfaces. Phys. Rev. Lett. 44 1680-1683.

Cowley JM (1964). The derivation of structural information from absorption effects in x-ray diffraction. Acta Cryst. 17 33-45.

Craven AJ, Gibson JM, Howie A, Spalding DR (1978). Study of single-electron excitations by electron microscopy. I. Image contrast from delocalized excitations. Phil. Mag. A38, 519-527.

Duncumb P (1962). Enhanced x-ray emission from extinction contours in a single-crystal gold film. Phil. Mag. 7 2101-2105.

Feldman LC, Mayer JW, Picraux ST (1982). Materials Analysis by Ion Channeling, Academic Press, New York.

Hall CR, Hirsch PB (1965). Effect of thermal diffuse scattering on propagation of high energy electrons through crystals. Proc. Roy. Soc. A 286 158-177.

Hall CR (1966). On the production of characteristic x-rays in thin metal crystals. Proc. Roy. Soc. A 295 140-163.

Hall CR, Hirsch PB, Booker, GR (1966). The effect of point defects on absorption of high energy electrons passing through crystals. Phil. Mag. 14 979-989.

Hirsch PB, Howie A, Whelan MJ (1962). On the production of x-rays in thin metal foils. Phil. Mag. 7 2095-2100.

Hirsch PB, Howie A, Nicholson RB, Pashley DW, Whelan MJ. (1977). Electron Microscopy of Thin Crystals (Krieger, NY) pp. 281-286.

Howie A (1966). Diffraction channeling of fast electrons and positions in crystals. Phil. Mag. 14 223-237.

Ichimiya A, Lehmpfuhl G (1978). Axial channeling in electron diffraction. Z. Naturforsch. 33a 269-281.

Jackson JD (1975). Classical Electrodynamics, 2nd Edition, Wiley, New York, p. 623.

Krishnan KM, Thomas G (1984). A generalization of atom location by channeling enhanced microanalysis. J. Microscopy 136 97-101.

Krishnan KM (1987). Atomic site and species determinations using channeling and related effects in analytical electron microscopy. Ultramicroscopy (in press).

Narayan J, Holland OW, Appleton BR (1983). Solid-phase-epitaxial growth and formation of metastable alloys in ion implanted silicon. J. Vac. Sci. Technol. B1 871-887.

Pennycook SJ, Howie A (1980). Study of single-electron excitations by electron microscopy II. Cathodoluminescence image contrast from localized energy transfers. Phil. Mag. A 41 809-827.

Pennycook SJ (1982). High resolution electron microscopy and microanalysis. Contemp. Phys. 23 371-400.

Pennycook SJ, Narayan J, Holland OW (1983). Formation of partially coherent antimony precipitates in ion-implanted thermally annealed silicon. J. Appl. Phys. 6875-6878.

Pennycook SJ, Narayan J, Holland OW (1984). Spatially resolved measurement of substitutional dopant concentrations in semiconductors. Appl. Phys. Lett. 44 547-549.

Pennycook SJ, Narayan J (1985). Atom location by axial-electron channeling analysis. Phys. Rev. Lett. 54 1543-1546.

Pennycook SJ, Berger SD, Culbertson RJ (1986). Elemental mapping with elastically scattered electrons. J. Micros. 144 229-249.

Self PG, Buseck PR (1983). Low-energy limit to channeling effects in the inelastic scattering of fast electrons. Phil. Mag. A48 L21-L26.

Spence JCH, Tafto J (1982). Atomic site and species determination using the channeling effect in electron diffraction. Scanning Electron Microsc. 1982; II: 523-531.

Spence J, Krivanek O, Tafto J, Disko M (1982). The crystallographic information in electron energy loss spectra. In: Electron Microscopy and Analysis 1981, (ed) Goringe MJ. Inst. Phys. Conf. Ser. No. 61, London 253-258.

Spence JCH, Tafto J (1983). ALCHEMI: a new technique for locating atoms in small crystals. J. Microsc. 130 147-154.

Spence JCH, Graham RJ, Shindo D (1986). Cold ALCHEMI: Impurity atom site location and the temperature dependence of dechanneling. MRS Symp. Proc. Vol. 62, 153-162.

Tafto J (1979). Channeling effects in electron induced x-ray emission from diatomic crystals. Z. Naturforsch. 34a 452-458.

Tafto J (1982). The cation-atom distribution in a (Cr, Fe, Al,Mg)$_3O_4$ spinel as revealed from the channeling effect in electron-induced x-ray emission. J. Appl. Cryst. 15 378-381.

Tafto J, Krivanek OL (1982). Site-specific valence determination by electron-energy loss spectroscopy. Phys. Rev. Lett. 48 560-563.

Tafto J, Spence JCH, Fejes P (1983). Crystal site location of dopants in semiconductors using a 100-keV electron probe. J. Appl. Phys. 54 5014-5015.

Tafto J (1983). Structure-factor phase information from two-beam electron diffraction. Phys. Rev. Lett. 51 654-657.

Treacy MMJ, Gibson JM (1982). On the detection of point defects in crystals using high-angle diffuse scattering in the STEM. Electron Microscopy and Analysis 1981, (ed) Goringe, MJ. Inst. Phys. Conf. Ser. No. 61, London, 263-266.

Van Dyck D (1985). Image calculations in high-resolution electron microscopy: problems, progress, and prospects. Advances in Electronics and Electron Physics, Academic Press, New York 65 295-355.

White CW, Wilson SR, Appleton BR, Young Jr., FW (1980). Supersaturated substitutional alloys formed by ion implantation and pulsed laser annealing of group-III and group-V dopants in silicon. J. Appl. Phys. 51 738-749.

Zaluzec NJ (1979). Quantitative x-ray microanalysis: instrumental considerations and applications to materials science. Introduction to Analytical Electron Microscopy, (eds) Hren JJ, Goldstein JI, Joy DC, Plenum, New York 121-167.

Discussion with Reviewers

J.C.H. Spence: Consider a crystal whose primitive unit cell contains several species on inequivalent sites. Which is more difficult:
a) to find planar orientations which separate candidate sites for a substitutional impurity onto separate planes also containing distinct reference atoms and belonging to a short stacking sequence, or b) to find axial orientations which separate them into distinct columns, each also containing separate reference atoms? (i.e. which is more crystallographically restrictive, axial or planar ALCHEMI? Our experience has been that the axial geometry gives a stronger, but less generally useful effect. If it can be used, it should.)

K.M. Krishnan: The author's conclusion that "axial channeling is highly advantageous compared to planar channeling" is not substantiated either by the contents of this review article or by the references cited therein (most of the references cited are on planar channeling). It is true that channeling effects have been generally shown to be enhanced in the axial case, but, as a practical tool, the planar method seems to have

demonstrated a wide variety of applications ranging from impurity site occupancy determination in complex sublattices to specific site valence determinations using ELS.

K.M. Krishnan: Can the author provide an example or cite references for the determinations of sublattice site occupations using axial channeling?

Author: Which geometry is more useful depends primarily on the structure of the specimen. For complex layer structures a planar geometry is most useful, but for other structures the axial geometry is advantageous, for example a monatomic matrix as studied here, for ordered alloys (text reference Bentley, 1986) and for minerals of the garnet structure (additional reference Otten and Buseck, 1987).

K.M. Krishnan: The criterion for perfect localization is somewhat arbitrarily determined in this paper. In the section "Determination of c-factors" it is $b^{rms} < 0.03$ nm. In Fig. 5 it is $b^{rms} < 0.04$ nm. Is there an objective criterion to determine this cut-off? How significant is this correction when compared to the routine errors observed in EDXS microanalysis?

Author: This correction can be much more significant than the routine errors observed in EDXS analysis, as can be seen from Fig. 5. Based on this figure we would suggest that "perfect" localization occurs for $d/b^{rms} \geq 30$. Delocalization effects become severe ($\gtrsim$50% reduction in channeling effect) when $d/b^{rms} \lesssim 5$, and we would not expect quantitative channeling analysis to be viable in such cases. Between these extremes the formulation presented here can provide a quantitative analysis (in any geometry).

J. Tafto: One might expect that the delocalization problem is more pronounced when many reflections are excited, because contributions from Fourier components with large g-vectors tend to localize the wavefield of the fast electrons. Generally, the number of excited reflections increases with increasing accelerating voltage, with increasing values of the Fourier potentials (i.e. large Z) and also for axial compared to planar channeling. Your result for As-L in Si for axial and planar channeling does not seem to support this statement. Neither does the comparison of the localization in the Si- and Ge-matrix as is discussed in the text. What is the accuracy of the delocalization factor c in Fig. 5, and thus the significance of the small differences you observe for Ge-L and As-L?

Author: The fine details in the fast electron intensity distribution are not expected to be important since the inner shell cross section as a function of impact parameter is quite slowly varying (text reference Jackson, 1975 and additional reference Ritchie, 1981). The lowest frequency Fourier components are therefore of primary importance in determining the reduction in channeling effect, which will occur when they are comparable to d. Hence the possibility that the c-factor curve (Fig. 5) may be a universal curve using the upper scale of d/b^{rms}, also the similar behavior of As-L in planar and axial geometries, and the similar behavior of the Si and Ge matrix.

The measurement of a c-factor depends both on the statistics of the spectra and also on how well the chosen off-axis direction represents a random direction. Many different beam tilts and specimen areas were analyzed and we estimate that the c-factors for Ge-L and As-L are accurate to ±0.04. We do not place any significance on the small differences observed.

A.J. Bourdillon: Presumably your c-factors can in principle be calculated for model systems and are consistent with Eq. 3. Does the energy dependence correspond with equivalent factors for various regions of the Bremsstrahlung?

Author: Electron-electron Bremsstrahlung involving those valence electrons n_v in spatially extended orbitals will appear delocalized at all emission energies, but this will be a small fraction $\sim n_v/Z^2$ of the total emission. The essential difference between the localization of Bremsstrahlung emission at energy E_i and the excitation of an inner shell of binding energy E_i is that the inner shell electron can be excited by all energy transfers $\Delta E > E_i$. Although there is a low probability of large energy transfers, the average impact parameter will be significantly smaller than for the Bremsstrahlung case. It can be estimated from

$$\overline{b^2}_{X ray} = \frac{\int_{E_i}^{E}\int_{0}^{\theta_c} \frac{d^2\sigma}{d\Delta E d\theta} b^2(\theta)\, d\theta\, d\Delta E}{\int_{E_i}^{E}\int_{0}^{\theta_c} \frac{d^2\sigma}{d\Delta E d\theta}\, d\theta\, d\Delta E} \quad (7)$$

where

$$\frac{d^2\sigma}{d\Delta E d\theta} = \frac{2\pi e^4}{\Delta E\ E} \frac{\theta}{(\theta^2+\theta_E^2)} \qquad \theta \leq \theta_c$$

$$= 0 \qquad \theta > \theta_c$$

(see additional reference Colliex et al., 1976)

$\theta_c = (\Delta E/E)^{1/2}$

$\theta_E = \Delta E/2E$

E_i = inner shell binding energy,

and from the uncertainty principle

$$b^2(\theta) \sim \frac{1}{\Delta k^2} = \left[\frac{2mE}{\hbar^2}(\theta^2+\theta_E^2)\right]^{-1} \quad (8)$$

Performing the angular integration alone results in Eq. 3 for a particular value of ΔE.
The full integration gives, for $E_i << E$:

$$b^{rms}_{X ray} = \frac{\hbar v}{E_i}\left(\ell n \frac{E}{E_i}\ \ln \frac{16E}{E_i}\right)^{-1/2} \quad (9)$$

which is smaller than the values given by Eq. 3 by a factor which ranges from 2.35 at E_i = 1 keV to 1.8 at E_i = 10 keV, for E = 100 keV.

Experimentally, we do observe a lower channeling effect for the Bremsstrahlung than expected from Fig. 5 at energies of 2-3 keV, consistent with reduced localization, but we also find a significant apparent localization even at energies below 1 keV (see Fig. 2b for example). This we attribute to Bremsstrahlung generated at regions remote from the beam (such as at the Cu specimen support ring or the Be specimen holder) by electrons scattered through large angles.

A. Howie: Strains in the surrounding crystal (usually tending to reduce the channeling effect) will probably be generated by coherent precipitates and even by isolated impurity atoms. Does the author see any way in which the experimentalist can test for and make allowance for these strain effects?

Author: It has normally been assumed in electron and in ion channeling that the dechanneling effect of defects and impurities is identical for both matrix and impurity x-ray emissions, and will therefore be factored out of a quantitative analysis. However, this is only true if there is a large number of scattering centers through the thickness of the specimen, and that each does not significantly alter the electron current distribution from what it would have been without the scattering center. Then, at any depth, the matrix and impurity atoms are sampled on average by the same electron distribution. In our case the precipitate density is sufficiently low that electrons scattered by one precipitate are unlikely to pass any further precipitates. Dechanneling involves the scattering of electrons or ions through large angles, in the electron case from Bloch states to plane wave states. The scattered flux will generate x-rays at the random rate on average, resulting in a reduced channeling effect from the column of material below a precipitate. The dopant would tend to appear more substitutional than it should, which is opposite to what we observe. In the electron case we also have the possibility of interband scattering between Bloch states which might conceivably result in a reversed impurity channeling effect if the transition occurred in the strain field as the electrons approached the precipitate. Fortunately, the significance of interband scattering can be easily assessed from the transmitted electron image. Figure 9 shows that under {220} planar channeling conditions used in the present study there is no strain contrast or depth-dependent precipitate contrast indicative of interband transitions (additional reference Howie and Hutchison, 1986). However, for <100> axial channeling there is clearly significant interband scattering. The axial case is characterized by the much smaller extinction distance of approximately 18 nm (estimated from Fig. 1) which is comparable with the size of the strain field.

It would certainly be desirable to study and quantify these effects but this would best be done in a well-characterized system where the strain fields and relative lattice displacements were known, perhaps the Cu-Co system.

J.C.H. Spence: The original ALCHEMI formulation was arranged so that it was not necessary to preserve the same electron beam intensity between different spectra. Your paper suggests that this is necessary in the method described here, yet your equations agree exactly with the original ones for perfect localization. Please clarify.

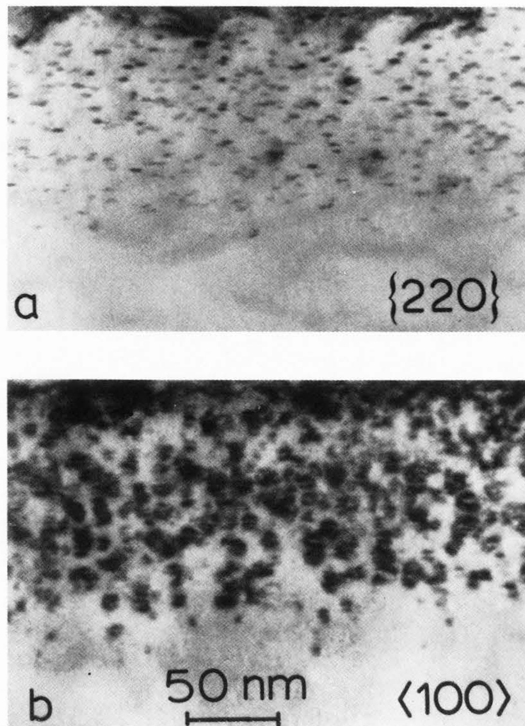

Fig. 9. Cross-section micrographs of Si implanted with a uniform concentration of Sb (8.8×10^{20} cm^{-3}) and annealed at 720°C for 20 min, in symmetric orientations corresponding to a) {220} planar channeling, b) <100> axial channeling.

Author: Equation 6 reduces to the ALCHEMI expression only in the case of perfect localization and substitutionality. Suppose we alter the measured individual channeling effects by a factor ρ, for example, by increasing the beam intensity for the random orientation, then the right hand side of Eq. 6 becomes

$$\frac{\frac{1}{C_X}\left(\rho \frac{N_X{}^C}{N_X{}^R} - 1\right) - F_S \frac{1}{C_B}\left(\rho \frac{N_B{}^C}{N_B{}^R} - 1\right)}{\frac{1}{C_A}\left(\rho \frac{N_A{}^C}{N_A{}^R} - 1\right) - \frac{1}{C_B}\left(\rho \frac{N_B{}^C}{N_B{}^R} - 1\right)}$$

Clearly, it is only under the original ALCHEMI assumptions of $C_X = C_A = C_B = F_S = 1$ that this reduces to

$$\frac{\rho \frac{N_X{}^C}{N_X{}^R} - \rho \frac{N_B{}^C}{N_B{}^R}}{\rho \frac{N_A{}^C}{N_A{}^R} - \rho \frac{N_B{}^C}{N_B{}^R}} = F_A$$

For general analysis with non-unity substitutional fractions, and/or delocalization correction, the channeling effects of individual elements must be measured, which requires the same electron beam intensity for both incident beam orientations.

J.C.H. Spence: How important are differences in x-ray absorption in the sample between your two orientations?
K.M. Krishnan: It might be instructive for the general reader if the author were to be more specific in comparing the errors introduced either in tilting the specimen or by tilting the incident beam. Could the author provide some estimate (i.e., percentages), for these errors and a rudimentary outline of the method used in determining them?
Author: We do not find appreciable absorption corrections in Si specimens. Changes in an absorption correction caused by tilting the specimen could be eliminated by tilting the incident electron beam, as done in the present study. In our experience, tilting the specimen can also cause a significant change in the absolute intensity of emitted X rays due to the change in path and path length through the specimen, particularly if large tilt angles are used as for the axial geometry. Since this formulation requires the same incident electron flux for the two orientations, this can lead to significant error. We normally use the beam tilting method using various "random" directions, but have not systematically studied the errors of each method.

K.M. Krishnan: The role of the tangential component of parallelism has been further investigated (Krishnan, Ultramicroscopy, in press). It has been shown, for the planar case, that best results are not always obtained for a convergent probe with a convergence angle less than the Bragg angle. The result is, of course, instrument dependent. Would the author expect "parallelism" to play a similar role in the axial formulation?
Author: We would indeed expect similar effects in the two geometries.

K.M. Krishnan: One cannot overemphasize the importance of the assumption of uniform distribution in the dopant through the thickness. For the ion-implanted samples (Fig. 4) the concentration seems to vary from ~10^{20} (10 nm) to 5×10^{21} (110 nm) for the thickness used. Could this have created significant errors in the determination of c-factors using the standards? Is it also possible, that because of the identical form of the thickness averaging in the standard and the unknown (both ion-implanted samples), the author was able to obtain such good agreement? In other words, would the results be different if the standard was an ion implanted one and the unknown material had a different impurity distribution? How can the effects of nonuniform impurity distribution be quantitatively assessed by inverting the specimen and repeating the axial channeling analysis?
Author: The As-implanted sample shown in Fig. 4 was used as a standard only in cross-section form in order to achieve a uniform depth profile

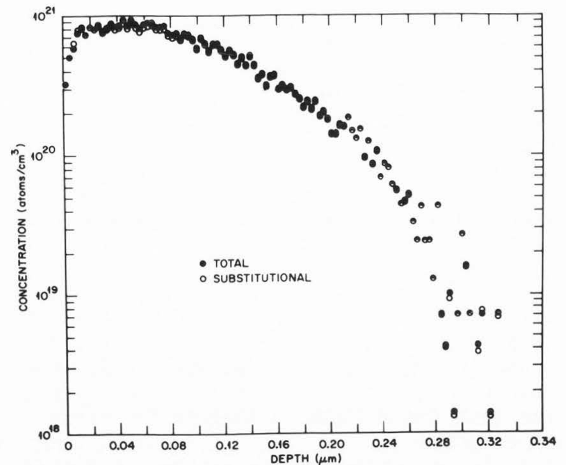

Fig. 10. Ion channeling analysis of Si implanted with Sb at various energies and doses to achieve a concentration approximately uniform from 10 to 110 nm in depth.

(see experimental section). The use of such a sample in plan view does indeed give significant errors as has been reported previously (additional reference Pennycook et al., 1984). For the Sb standards, both cross section and plan view samples were used, but in the plan view case a multiple implant scheme was used to give the profile shown in Fig. 10, which is approximately uniform from 10 to 110 nm in depth. The effect of nonuniformities in the profile was assessed by inverting the specimen. Although there is no simple way to quantitatively assess these effects, if no change is detected on inverting the specimen any effects due to a nonuniform distribution must be less than the experimental error in the channeling effect. We do not believe there are significant errors in the c-factors determined.

Additional References

Colliex C, Cosslett VE, Leapman RD, Trebbia P. (1976). Contribution of electron energy loss spectroscopy to the development of analytical electron microscopy, Ultramicroscopy 1 301-315.

Howie A, Hutchison JL (1986). Comparison of the diffraction contrast and the slice method for image computation. J. Microscopy 142 131-139.

Otten MT, Buseck PR (1987). Axial ALCHEMI: a method for assessing crystallographic site occupancies in garnet. Nature (in press).

Pennycook SJ, Narayan J, Holland OW (1984). Dopant site location by electron channeling in ion implanting silicon. Mat. Res. Soc. Symp. Proc. 31 97-104.

Ritchie RH (1981). Quantal aspects of the spatial resolution of energy-loss measurements in electron microscopy. Philos. Mag. A44 931-942.